Supplementary Material Available: Listings of anisotropic thermal parameters (Tables 1S, 4S, 7S, 10S, 13S, 16S, and 19S) and hydrogen atom coordinates (Tables 2S, 5S, 8S, 11S, 14S, 17S, and 20S) for I-VII and bond distances and angles for V (Tables S22, S23) and crystal packing diagrams for I-VII (Figures S1-S7) (18 pages); listings of observed and calculated structure factors (Tables 3S, 6S, 9S, 12S, 15S, 18S, and 21S) for I-VII (71 pages). Ordering information is given on any current masthead page.

Contribution from the Department of Chemistry,
University of Delaware, Newark, Delaware 19716

Thermal Decomposition of Energetic Materials. 30. Thermolysis of Energetic Metal-Nitraminato Complexes under Conditions That Simulate Combustion

S. F. Palopoli and T. B. Brill*

Received February 3, 1988

The thermal decomposition of six energetic nitraminato complexes of Cu(II), Pd(II) and Ni(II) was investigated at 5 °C/min by IR spectroscopy and DSC and at 100 °C/s (to simulate combustion) by rapid-scan infrared spectroscopy. The objective was to correlate, insofar as possible, the structure and bonding of the parent complex to the decomposition behavior and products. The metal-nitraminato complexes decompose very rapidly. The gases liberated are farther along toward final combustion products than is the case with most organic nitramines subjected to the same thermal conditions. The thermolysis properties of $M(NH_3)_2[N(NO_2)(CH_2)_2N(NO_2)]$ (M = Cu, Pd) complexes can be understood in terms of the relative strengths of the metal-nitrogen bond. Most of the NH_3 is retained by the Pd complex in the condensed phase while decomposition occurs, whereas more of the NH_3 is released to the gas phase in advance of decomposition by the Cu complex. There is circumstantial evidence that the high potential for forming $^{\bullet}H$ in the ammine complexes drives the thermolysis farther along toward the final, thermodynamically stable products. The Ni(II) complexes were more difficult to characterize because the thermal stimulus exploded the samples.

Introduction

The objective of this research program has been to uncover relationships between the bonding and molecular structure of selected molecules and the distribution of gas products evolved under conditions that simulate ignition and combustion. New thermolysis techniques have been developed for this work that employ rapid-scanning infrared spectroscopy as the principal analytical tool.[1,2] The experiments are designed to give a phenomenological understanding of thermolysis mechanisms as opposed to kinetic data. This is because the processes taking place are multistep, physicochemical in nature, and nonisothermal and involve the heterogeneous gas and condensed phase. Despite the complexity of the events and the experimental trade-offs that studies of this type require, much new insight has been achieved. This program has been directed mainly at energetic organic molecules containing $N-NO_2$,[1,3-15] $O-NO_2$,[16] and $C-NO_2$[3,5,6,17-20] linkages: azides,[1,2,15,21] furazans,[22] furoxans,[8] nitrate salts,[20,23,25] and perchlorate salts.[24] Some guidelines have emerged on the factors influencing the tendency of these compounds to liberate NO_2,[7,10] HONO,[9] N_2O,[6,13] NO,[9] HNO_3,[20,23-25] CH_2O,[6,13] NH_3,[20] and CH_4[21] upon high rate thermolysis. The influence of cyclization of linear nitramines on the thermolysis[11] and condensed-phase[26] properties was analyzed. Some of the chemistry that occurs when decomposition transits to deflagration was captured in real time in the same experiment.[18] The effect of pressure on identity of the first observed gas products was analyzed.[27]

Successful studies of this type require rapid, real-time measurements because the gas products are often quite reactive. If certain products are missed, then the relationship between the observed gas products and the structure and bonding of the parent molecule may not be decipherable. Even with all of these precautions taken into account, only a few of the products come from primary decomposition reactions. On the other hand, the species have sufficient stability to exist in concentrations to control the various flames of a combusting material. These products thus strongly influence the combustion properties. Given the complexity of the decomposition/ignition/combustion process, the conclusions that can be drawn from our studies are largely qualitative. However, they present new insights into the thermal degradation reactions of materials under conditions that approach combustion.

This paper describes the first real-time, in situ, gas product speciation studies of metal complexes subjected to high heating rates and pressures. Our objective was to uncover some of the relationships between the structure and bonding in the parent energetic metal complexes and their decomposition products. Both slow and fast thermolysis experiments were conducted. The compounds investigated are the metal-nitraminato complexes whose syntheses and structures are described in the preceding paper in this issue. Some of these compounds might be potentially

(1) Oyumi, Y.; Brill, T. B. *Combust. Flame* **1985**, *62*, 213.
(2) Cronin, J. T.; Brill, T. B. *Appl. Spectrosc.* **1987**, *41*, 1147.
(3) Oyumi, Y.; Brill, T. B. *Combust. Flame* **1985**, *62*, 225.
(4) Oyumi, Y.; Brill, T. B. *Combust. Flame* **1985**, *62*, 233.
(5) Oyumi, Y.; Brill, T. B.; Rheingold, A. L. *J. Phys. Chem.* **1985**, *89*, 4824.
(6) Oyumi, Y.; Rheingold, A. L.; Brill, T. B. *J. Phys. Chem.* **1986**, *90*, 2526.
(7) Brill, T. B.; Oyumi, Y. *J. Phys. Chem.* **1986**, *90*, 2679.
(8) Oyumi, Y.; Rheingold, A. L.; Brill, T. B. *J. Phys. Chem.* **1986**, *90*, 4686.
(9) Brill, T. B.; Oyumi, Y. *J. Phys. Chem.* **1986**, *90*, 6848.
(10) Oyumi, Y.; Rheingold, A. L.; Brill, T. B. *Propellants Explos. Pyrotech.* **1987**, *12*, 1.
(11) Oyumi, Y.; Brill, T. B.; Rheingold, A. L. *Thermochim. Acta* **1987**, *114*, 209.
(12) Oyumi, Y.; Rheingold, A. L.; Brill, T. B. *J. Phys. Chem.* **1987**, *91*, 920.
(13) Oyumi, Y.; Brill, T. B. *Combust. Flame* **1987**, *67*, 121.
(14) Palopoli, S. F.; Brill, T. B. *Combust. Flame* **1988**, *72*, 153.
(15) Brill, T. B.; Karpowicz, R. J.; Haller, T. M.; Rheingold, A. L. *J. Phys. Chem.* **1984**, *88*, 4139.
(16) Oyumi, Y.; Brill, T. B. *Combust. Flame* **1986**, *66*, 9.
(17) Oyumi, Y.; Brill, T. B. *Combust. Flame* **1986**, *65*, 103.
(18) Oyumi, Y.; Brill, T. B. *Propellants Explos. Pyrotech.* **1986**, *11*, 35.
(19) Oyumi, Y.; Rheingold, A. L.; Brill, T. B. *Propellants Explos. Pyrotech.* **1987**, *12*, 46.
(20) Oyumi, Y.; Brill, T. B. *J. Phys. Chem.* **1987**, *91*, 3657.
(21) Oyumi, Y.; Brill, T. B. *Combust. Flame* **1986**, *65*, 127.
(22) Oyumi, Y.; Brill, T. B. *Combust. Flame* **1986**, *65*, 313.
(23) Oyumi, Y.; Brill, T. B.; Rheingold, A. L.; Lowe-Ma, C. *J. Phys. Chem.* **1985**, *89*, 2309.
(24) Oyumi, Y.; Brill, T. B. *J. Phys. Chem.* **1985**, *89*, 4325.
(25) Cronin, J. T.; Brill, T. B. *J. Phys. Chem.* **1986**, *90*, 178.
(26) Oyumi, Y.; Brill, T. B. *Thermochim. Acta* **1987**, *116*, 125.
(27) Oyumi, Y.; Brill, T. B. *Combust. Flame* **1987**, *68*, 209.

0020-1669/88/1327-2971$01.50/0

useful as additives to tailor the burn rate of solid rocket propellants, especially propellants in which an organic nitramine is the monopropellant. However, the techniques and knowledge gained have potential for application far beyond the specific compounds investigated here. For example, there is a growing interest in understanding the thermolysis of metal complexes that could form new solid-state materials.

Experimental Section

The synthesis and characterization of the metal complexes studied in this project are described in the preceding paper in this issue. *Caution*! All of the compounds inflame or explode when heated rapidly on a hot plate. Explosions also occur on hammer impact. Therefore, the sample size was kept as small as possible, and due care was taken in handling the materials.

IR Spectroscopy Studies. IR spectra were recorded on a Nicolet 60SX FTIR spectrometer equipped with an MCT-B detector. Transmission spectra of the condensed phase were recorded as a function of temperature by using a cell described before.[28] A dusting of neat polycrystalline material was burnished onto an NaCl plate, which was covered with a second plate and mounted in the cell. A thermocouple in contact with the NaCl plate permitted temperature measurements to ±2 °C accuracy. A heating rate of 5 °C/min was used. The spectra were accumulated at 2-cm^{-1} resolution, and transformed after coadding 32 scans.

The home-built cell, experimental procedures, and data analysis practices for high heating rate thermolysis studies with rapid-scan infrared spectroscopy are described in detail elsewhere.[1] The parameters of this cell have been thoroughly explored with respect to their influence on the thermolysis process. Only an overview of pertainent details will be given here. In a typical experiment 1 or 2 mg of powdered polycrystalline sample was thinly spread on the nichrome ribbon filament. The IR beam passed several millimeters above the long axis of this filament. Potential catalytic effects of this filament surface on the decomposition reactions have been investigated with energetic materials whose decomposition is known to be especially sensitive to catalysis.[29] Under the conditions used, the surface of the filament was found to have little effect on the nature of the gas products or their relative concentrations. The temperature profile of the filament as a function of time was measured by spot-welding a thermocouple to the base of the filament and recording its output on a storage oscilloscope. The range of heating rates available was 20–800 °C/s. Voltage was applied to the filament for 10 s. Essentially linear ramp heating at rates described in the text occurred for 1–4 s depending on the heating rate chosen. The heating rate then diminished as the filament approached the final temperature. The static Ar pressure in the cell was adjusted as desired between 1 and 1000 psi of Ar before the filament was fired. The spectrometer was normally set to scan at 10 scans/s, 2 spectra/file, and 4-cm^{-1} resolution.

When all of the above experimental variables were adjusted as desired, the filament was fired and a fast-acting shutter blocking the IR beam was simultaneously opened. The first interferogram corresponded to the onset of heating. As the sample is rapidly heated, the first gas products appeared in the IR beam. The time of appearance, of course, depends on the temperature at which the sample decomposes and the heating rate. Since the gas products evolve into relatively cooler Ar gas, their reactions are slowed during the 200-ms spectral frames. Within several seconds the reactions involving the parent molecule are over and mixing is complete.

Quantitation of the gas products was accomplished by measuring the intensities of characteristic absorptions for each product and taking the ratio of these values to the absolute intensities.[1] These ratios were then placed on a percent scale to yield the relative percent composition of each product. Plots of relative percent concentration of the gas products versus pressure were constructed by performing the above experiment at various different static Ar pressures and quantifying the first observed products.[27] For this experiment an otherwise constant set of experimental variables was maintained so that the effect of pressure alone on the identities and concentrations of the gases could be isolated. H_2O was not included in any of the concentration profiles because, although it was liberated from almost all of the complexes, its rotation–vibration fine structure made quantitation difficult. HNCO was frequently a thermolysis product of nitramines.[1,3–15] It was liberated by all of the metal complexes except the triammine(5-nitraminotetrazolato)nickel(II) dimer. Unfortunately, no IR absolute intensities are available for HNCO. Thermolysis of (ethylenediamine)bis(methylnitraminato)copper(II), and poly(diammine(ethylenedinitraminato)copper(II)) produces several comparatively weak IR absorptions that could not be assigned or could only be tentatively assigned to known compounds. Exhaustive effort was expended on attempts to assign these unknown absorptions. It would have been gratifying to identify every product, but the conclusions that will be drawn about the thermolysis data would not be greatly influenced by this knowledge.

Differential Scanning Calorimetry. DSC measurements were made on a Dupont Instruments 990 DSC instrument using an N_2 flow rate of 75 cm^3/min, a heating rate of 5 °C/min, and crimped P-E sample pans. The initial temperature was obtained by extrapolating a straight line from the steepest point of heat release to the base line.

Nitramine Decomposition

Because of their use as chemical rocket propellants and explosives, considerable effort has been made to understand the thermal decomposition of organic nitramines.[1,3–15,30–32] Two multistep reactions leading to products that contribute to combustion in the gas phase are summarized by (1) and (2). Here,

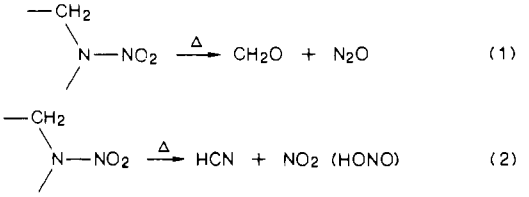

(1) involves N–N bond retention while (2) involves N–N bond homolysis. Other reaction pathways are not precluded, but (1) and (2) are widely accepted as being the dominant ones. These two reactions frequently compete so that all of the products are found. The structure and composition of the parent nitramine molecule, the final temperature and rate of heating during thermolysis, and, possibly, the phase contribute to determining the proportion of degradation that occurs by (1) and (2). Frequently, the products of (1) and (2) react before detection, but the products of these later stage reactions can be indicative of what has taken place. Experience has shown that rapid heating rates and rapid, real-time diagnostics are needed to develop the picture.[1–27] Therefore, the gas products generated by the high heating rate thermolysis of metal–nitraminato complexes were characterized by rapid, real-time, in-situ IR diagnostics. The results appear to be interpretable in the same context as those for organic nitramines when the influence of the metal–nitrogen bond strength is taken into account.

Comparison of $M(NH_3)_2[N(NO_2)(CH_2)_2N(NO_2)]$ (M = Cu, Pd)

The contribution of differences in the electron distribution in the parent molecule to the gas products liberated by thermolysis is evident when poly-$Cu(NH_3)_2[N(NO_2)(CH_2)_2N(NO_2)]$ (**1**) is compared to $Pd(NH_3)_2[N(NO_2)(CH_2)_2N(NO_2)]$ (**2**). The

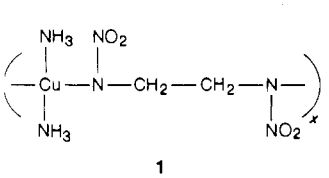

1

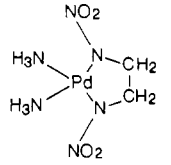

2

(28) Karpowicz, R. J.; Brill, T. B. *Appl. Spectrosc.* **1983**, *37*, 79.
(29) Cronin, J. T.; Brill, T. B. *Combust. Flame*, in press.
(30) Shackelford, S. A.; Coolidge, M. A.; Goshgarian, B. B.; Loving, B. A.; Rogers, R. N.; Janney, J. L.; Ebinger, M. H. *J. Phys. Chem.* **1985**, *89*, 3118.
(31) Bulusu, S.; Weinstein, D. I.; Autera, J. R.; Velicky, R. W. *J. Phys. Chem.* **1986**, *90*, 4121.
(32) For research, discussion and reviews see: (a) Schroeder, M. A. *CPIA Publ.* **1979**, *2* (*No. 308*), 17. (b) Schroeder, M. A. Presented at the *21st JANNAF* Combustion Meeting, Lawed, MD, Oct 1984. (c) Dubovitskii, I. I.; Korsunski, B. L. *Russ. Chem. Rev.* (*Engl. Transl.*) **1981**, *50*, 958. (d) Boggs, T. L. *Prog. Astronaut. Aeronaut.* **1984**, *90*, 121. (e) Shaw, R.; Walker, F. E. *J. Phys. Chem.* **1977**, *81*, 2572. (f) McCarty, K. P. AFRPL-76-59; Air Force Rocket Propulsion Laboratory: Edwards AFB, CA, 1976. (g) Ben-Reuven, M., Caveny, L. H. MAE Report 1455, Jan 1980, Princeton, NJ, (AD-4085650). (h) Zeman, S. *Thermochim. Acta* **1981**, *49*, 219. (i) Fifer, R. A. *Prog. Aeronaut. Astronaut.* **1984**, *90*, 177. (j) Cohen, N. S.; Lo, G. A.; Crowley, J. C. *AIAA J.* **1985**, *23*, 276.

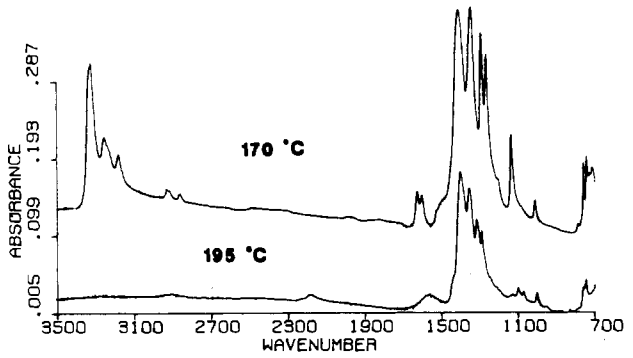

Figure 1. IR spectrum of a thin polycrystalline film of poly-Cu-$(NH_3)_2[N(NO_2)(CH_2)_2N(NO_2)]$ (**1**) on an NaCl plate below the decomposition temperature (170 °C) and above the decomposition temperature (195 °C). Note the loss of the absorptions associated with NH_3 (3100–3400 cm^{-1}) without much alternation in the gross features of the nitramine absorptions.

Table I. Differential Scanning Calorimetry Data for the Decomposition of Metal–Nitraminato Complexes

compd	T_{onset},[a] °C	T_{max},[b] °C	ΔH_{exo},[c] J/g
1	213	221	2530
2	246	274	1730
3	177	181	2370
4	203	207	2200
α-**5**	232	269	2390
β-**5**	229	270	2360

[a] Error = ±5. [b] Error = ±1. [c] Error = ±100.

compositions of these compounds are the same but the structures are different.[33] However, the difference in the structure does not appear to be central to the differences in the thermolysis results. The data are most readily understood in terms of the relative strength of the Cu–N and Pd–N bond.

Figure 1 shows the transmission IR spectrum of a thin film of **1** heated at 5 °C/min at 170 °C (below the reaction temperature) and at 195 °C (above the reaction temperature). The NH_3 modes disappear between 177 and 183 °C, whereas the modes of the $N(NO_2)(CH_2)_2N(NO_2)^{2-}$ ligand (hereafter called EDNA-2H) change very little. In accordance with this, when the gas phase above a sample of **1** heated at 5 °C/min is monitored, a small amount of NH_3 can be detected beginning at about 150 °C. It builds to a significant concentration above about 180 °C, before other decomposition products appear. By DSC, the temperature of the onset of the measured decomposition exotherm is about 213 °C (Table I), which is somewhat higher than the decomposition temperature measured by IR methods. The different sample conditions and observables in the IR and DSC experiments sometimes produce a difference in the temperature that is associated with the same event.[6] With the loss of NH_3 from the complex, it is possible that (EDNA-2H) becomes an O- and N-bound four-membered chelate toward the Cu atom. This mode of bonding has precedence in nickel–nitraminato complexes.[34]

The palladium complex, **2**, thermalized in the same manner as **1**, yields a different result. The vibrational modes for coordinated NH_3 decrease in intensity and shift at the same time the modes assignable to EDNA-2H change. The pronounced change occurs at about 230 °C, which is substantially above that for **1**. By DSC the temperature of the onset of the decomposition exotherm is about 274 °C.

The above results are consistent with the fact that Pd-N bonds are stronger than the analogous Cu–N bonds.[35,36] As a result,

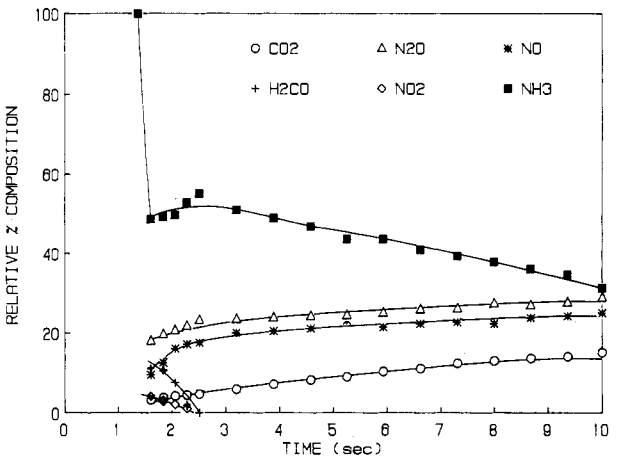

Figure 2. Quantified gas products in relative percent concentration vs time from the thermolysis of poly-Cu$(NH_3)_2[N(NO_2)(CH_2)_2N(NO_2)]$ (**1**) heated at 112 °C/s under 7.5 psi of Ar. H_2O, HNCO, and IR-inactive products are not included.

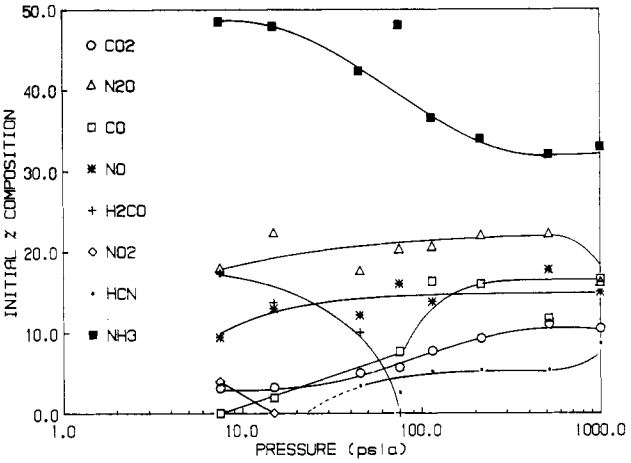

Figure 3. Relative percent concentrations of the initially detected (first 200 ms of thermolysis) gas products from **1** as a function of the static applied Ar gas pressure. The sample was heated at a rate of 110 °C/s at each pressure.

heterolysis of the Cu–NH_3 bond is expected to occur at a lower temperature than heterolysis of the Pd–NH_3 bond. In keeping with this, a large amount of NH_3 is detected in the gas phase by IR spectroscopy in advance of the other decomposition products when **1** is slowly pyrolyzed. A much smaller amount of NH_3(g) is liberated by the pyrolysis of **2**.

The above information can be applied to the decomposition pathways of the whole molecule under conditions that simulate combustion when high heating rates are used. Figure 2 shows the relative percent concentrations of the quantified gas products versus time when 2 mg of **1** is ramp heated at 112 °C/s under 7.5 psi of Ar to a final filament temperature of 610 °C. The first detected gas products are usually the most informative because the reactions involving the parent molecule in the condensed phase are essentially finished within a few seconds. Note that the dominant first detected product is NH_3, which undoubtedly is produced by Cu–NH_3 bond heterolysis. Within 0.2 s following the appearance of NH_3, gases formed by the decomposition of the EDNA-2H ligand appear. The most reactive gases among these products are CH_2O and NO_2, which quickly decompose as a result of further heterogeneous gas-phase/condensed-phase reactions and purely gas-phase reactions. The concentrations of these two products depend on the applied pressure. For many energetic organic compounds, the static Ar pressure in the cell exerts a strong influence on the identity and concentration of the gas products detected within 0.2 s of the onset of thermolysis.[27] The pattern is best summarized by plotting the initial percent concentrations of the gases versus pressure as shown in Figure

(33) Palopoli, S. F.; Geib, S. J.; Rheingold, A. L.; Brill, T. B. *Inorg. Chem.*, preceding paper in this issue.
(34) Liebig, D. M.; Robertson, J. H.; Truter, M. R. *J. Chem. Soc. A* **1966**, 879.
(35) Rasmussen, L.; Jørgensen, C. K. *Acta Chem. Scand.* **1968**, *22*, 2313.
(36) Mercier, R. C.; Bonnet, M.; Paris, M. R. *Bull. Soc. Chim. Fr.* **1965**, 2926.

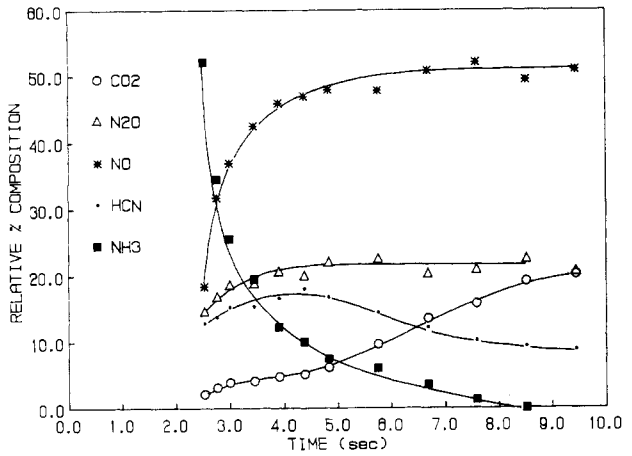

Figure 4. Quantified gas products in relative percent concentration vs time from the thermolysis of $Pd(NH_3)_2[N(NO_2)(CH_2)_2N(NO_2)]$ (**2**) heated at 110 °C/s under 7.5 psi of Ar. H_2O, HNCO, and IR-inactive products are not included.

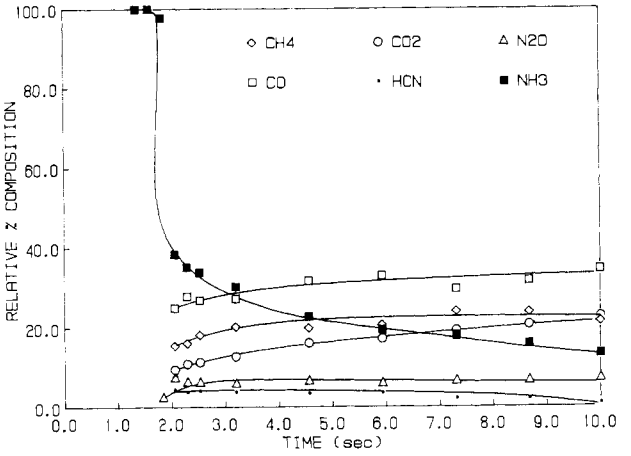

Figure 5. Quantified gas products in relative percent concentration vs time from the thermolysis of *trans*-$Cu(NH_3)_2[N(NO_2)CH_3]_2$ (**3**) heated at 65 °C/s under 15 psi of Ar. HNCO and IR-inactive products are not quantified.

3. Because the other experimental variables were held as constant as possible in constructing Figure 3, the pressure is the dominant variable. At lower pressure the most reactive gas products, NO_2 and CH_2O, are able to diffuse several millimeters away from the condensed phase and into the IR beam where they are detected. As the pressure is raised, the rate of diffusion of these gases is reduced so that they are able to react further with themselves and with the condensed phase before reaching the IR beam.[27] Hence, products that are farther along in the decomposition scheme dominate at higher pressure.

A comparison of the details of the thermal decomposition products of the nitramine fragment of **1** and EDNA[13] cannot be made because they have different compositions at the energetic site. However, the broad differences are striking. It is noteworthy that CH_2O is not detected from the thermolysis of EDNA,[13] but is from **1**, suggesting that reaction 1 is important for compound **1**. However, this is not the only thermolysis pathway because **1** produces less N_2O and more NO than does EDNA. This is consistent with the formation of an undetected amount of the reactive product HONO from the reaction of $^{\bullet}NO_2$ (from N–N bond homolysis) and $^{\bullet}H$[9] (possibly from NH_3 thermolysis). HONO decomposes to $^{\bullet}NO_2$, $^{\bullet}NO$ and H_2O. Thus, the presence of NH_3 may strongly influence the distribution of the decomposition pathways 1 and 2 of the EDNA-2H ligand by providing a major source of $^{\bullet}H$. In support of N–N bond homolysis in **1**, HCN has a much greater concentration than exists from EDNA. HCN probably forms from the H_2CN fragment of the nitramine via pathway 2.[37] Black CuO appears to be the solid residue that remains on the filament following complete thermolysis of **1**.

The fast thermolysis results for **1** contrast with those for **2**. The slow heating rate results discussed above suggest that the NH_3 ligands of **2** are retained in the condensed phase for a longer period of time than for **1**. In accordance with this, $NH_3(g)$ is released simultaneously with other products during the fast decomposition of **2** as opposed to earlier with **1**. Figure 4 shows the concentration versus time profile for **2** heated at 110 °C/s. The concentration of NH_3 never reaches that generated by **1**. As a result, a considerable amount of NH_3 is retained in the condensed phase where it can participate in the thermolysis reactions of the EDNA-2H ligand. Because the Pd–N bonds are stronger than Cu–N bonds, it seems logical that the $N–NO_2$ homolysis pathway giving NO_2 will occur to a greater extent in **2** than a pathway that involves splitting the Pd–N bond, retaining the N–N bond, and producing N_2O. However, the presence of $^{\bullet}H$ in the condensed phase would consume $^{\bullet}NO_2$ by forming HONO. HONO in turn degrades to produce $^{\bullet}NO$ ($^{\bullet}NO_2 + {}^{\bullet}H \rightarrow {}^{\bullet}NO + {}^{\bullet}OH$ and $2HONO \rightarrow {}^{\bullet}NO_2 + {}^{\bullet}NO + H_2O$). Thus, it might be anticipated NO will be present in much higher concentration from **2** than **1**. A comparison of the data in Figures 2 and 4 reveals this to be the case. A gray-black residue, probably PdO, is the solid that remains upon thermolysis.

(37) Morgan, C. U.; Beyer, R. A. *Combust. Flame* **1979**, *36*, 99.

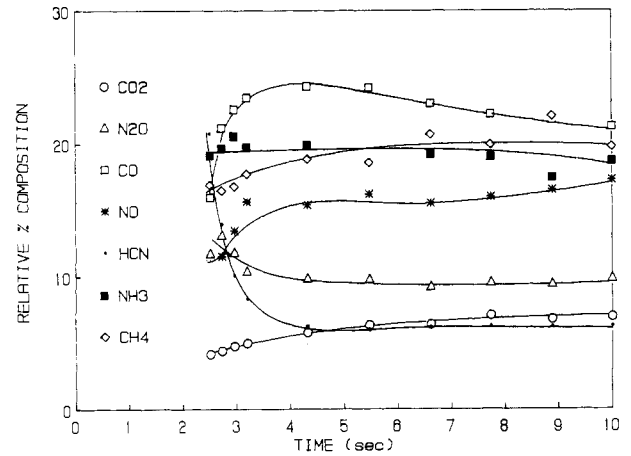

Figure 6. Quantified gas products in relative percent concentration vs time from the thermolysis of $Cu(NH_2CH_2CH_2NH_2)[N(NO_2)CH_3]_2$ (**4**) heated at 65 °C/s under 15 psi of Ar. One or more minor unidentified products along with some CH_3OH, H_2O, and C_2H_4 are not included in this plot.

Different heating rates in the 80–180 °C/s range and pressure differences in the 7.5–1000 psi of Ar range have very little effect on the relative concentrations of the products from **2**.

In summary, the results for **1** and **2** illustrate how the bonding properties of the parent molecule probably influence the gas thermolysis products that are available for ignition/combustion. The difference appears to originate in the trend of the metal–nitrogen bond strength (Pd–N > Cu–N).

Copper–Nitraminato Complexes

The coordination sphere of Cu(II) in **1** and *trans*-diammine-bis(methylnitraminato)copper(II) (**3**) closely resemble one another,

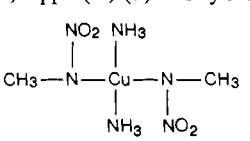

3

but the composition differs by 2 H/formula unit. Some interesting differences result upon high rate thermolysis. The relatively weak Cu–N bonds allow for NH_3 to be released in advance of the other decomposition products (see Figure 2 for the thermolysis products of **1** and Figure 5 for the products of **3**). However, a small amount of methylnitramine, $CH_3N(H)NO_2$, is evolved at the outset from

3, implying that the Cu–N(nitraminato) bond fission and •H transfer must take place to some extent. 3 then vigorously decomposes, producing a variety of stable gas products. After these products form there are few further reactions because the concentrations display little time-dependent behavior. CH_4 is a product as is frequently the case for molecules containing $-CH_3$ groups.[21] On the basis of the findings above, (ethylenediamine)bis(methylnitraminato)copper(II) (4) might be expected

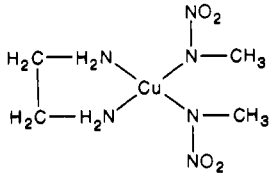

4

to display major differences in the gas product distributions because NH_3 is not available from simple Cu–NH_3 heterolysis. Figure 6 shows the relative percent concentrations of the gas products versus time for the thermolysis of 4 heated at 60 °C/s under 15 psi of Ar. The observations can be compared to those in Figure 5 for 3. As with 3, 4 releases a small amount of methylnitramine before the ligand fragments appear.

Because of the lower oxygen content, 4 is less energetic and more thermally stable than 3 (Table I). This may be responsible for the higher concentration of nitrogen oxides from 4 compared to 3. The lower oxygen content of 4 compared to 3 may also be responsible for why metallic copper rather than CuO is formed from the thermolysis of 4.

The complexity of the thermolysis reactions in 4, are evident by the fact that NH_3 is released even though a multistep reaction is required for its formation. 4 also generates CH_3OH, C_2H_4, and one or more transient products having relatively low absorbance values. Considerable effort was expended in an attempt to identify the unknown(s). Given that numerous reactions obviously occur during the thermolysis of 4, additional insight is difficult to acquire.

Nickel–Nitraminato Complexes

The connection between structure and bonding in nickel–nitraminato complexes and their high-rate thermolysis characteristics was complicated by the fact that, in all cases, ignition or an explosion took place when the decomposition of the nitraminato ligand became involved. We do not believe that this is caused by a characteristic difference between Ni(II) complexes of nitramines and those of Cu(II) and Pd(II). More likely it is tied to the ligand formulation and the composition of the complex at the exotherm.

The condensed-phase decomposition of two polymorphs of tetraaqua(ethylenedinitraminato)nickel(II) (5) was investigated

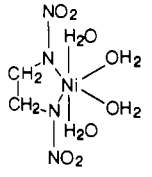

5

by IR, DSC, and TGA[38] methods at a heating rate of 5 °C/min. Both polymorphs are partially dehydrated upon heating to 125 °C. The IR spectra indicate that the dehydration product is the same for both polymorphs. This explains why the values for the temperature and the ΔH of the decomposition exotherm are essentially the same (Table I). By TGA, three H_2O molecules per formula unit are liberated before the nitramine molecules degrade. This was confirmed by monitoring the gas phase during the decomposition of these samples at low heating rates (5 °C/min). Only H_2O is liberated below 140 °C. A sample of the dehydrated product detonated during CHN analysis. Plausible structures for the dehydration product are 6 or 7. The green color of the product

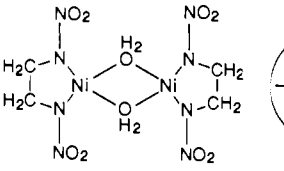

6

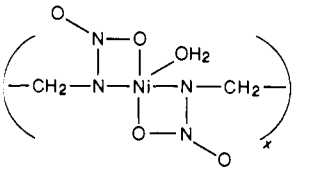

7

is more consistent with a five coordinate polymeric Ni(II) complex (7) with a bidentate nitramine ligand[34] than for the square-planar Ni(II) in 6. Either product would be expected to be highly energetic.

The dehydration product of 5 is also obtained by evacuation at 10^{-3} Torr for 48 h. Upon rehydration the α-polymorph is obtained. In one instance rehydration resulted in an "intermediate", probably amorphous, phase (IR spectrum similar to the "broadened" aqueous solution spectrum of 5). Mechanical stimulation (friction) converted this phase to the α-polymorph. The DSC of the α-polymorph shows a broad ($\Delta T_{base} \sim 45$ °C) endotherm for the dehydration at 125 °C. A similar endotherm at ~125 °C is observed for the β-polymorph. However, in addition, a sharp endotherm (at 110 °C) is observed superposed on the leading edge of the broad endotherm. We believe this corresponds to an order–disorder transition. An IR spectrum of the β-polymorph sampled from the crimped DSC pan after the first endotherm is the same as the spectrum of the amorphous phase described above.

Thermolysis of complex 8, bis[triammine(5-nitraminotetrazolato)nickel(II)], resulted in the liberation of some of the NH_3. This product is followed by the virtually instantaneous

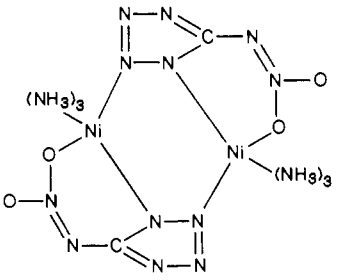

8

formation of CO_2. N_2 is undoubtedly produced but is not detected by IR spectroscopy. Because so few products from 8 can be analyzed by IR spectroscopy and the reaction occurs so rapidly, very little can be said about its decomposition mechanism. The tetrazole ring probably explosively decomposed.

In summary, this new type of investigation of energetic metal complexes experiencing a thermal stimulus that simulates combustion helps define some aspects of the fast thermal decomposition process in selected complexes.

The distribution of nitrogen oxide and carbon oxide gas products is further along toward the thermodynamically stable products of combustion than it is with the organic homologues of the ligands. Hence, the global reaction rate appears to be faster and autocatalysis is greater with the metal complexes. The dominant molecular parameter of the parent complex in determining the gases released appears to be the metal–nitrogen bond strength. Secondarily, this difference influences the amount of •H in the condensed phase. The availability of •H clearly affects the decomposition reactions.

The qualitative and phenomenological description given here presses the limit of experimental capability. Thus many aspects of the thermolysis of these compounds remain to be answered. For example, it is not known whether coordinative unsaturation of the metal is an important factor in accelerating the thermolysis reactions or whether the metal atom contributes to •H transfer.

(38) TGA analyses were performed by R. A. Biddle at Morton-Thiokol, Inc., on a DuPont 1090 TGA instrument. Samples were heated at 5 °C/min under an Ar purge (50 cm³/min).

Therefore, we regard this paper as only a first step toward understanding the chemistry of metal complexes that deflagrate or explode.

Acknowledgment. We are grateful to Morton-Thiokol, Inc., for financial support of this research on an independent research and development program and to the Air Force Office of Scientific Research, Aerospace Sciences, with whose support the spectrometer and analytical procedures were developed. We thank Drs. David A. Flanigan, Winston Brundige, Ernest Sutton, and Richard Biddle (Morton-Thiokol) for encouragement and discussions during the course of this work.

Contribution from the Departamentos de Cristalografia y Mineralogia y de Quimica Inorgânica, Universidad del Pais Vasco, Apartado 644, 48080 Bilbao, Spain, Sektion für Röntgen- und Elektronenbeugung, Universität Ulm, Oberer Eselsberg, D-7900 Ulm, West Germany, Departamento de Quimica Inorgânica, Universidad de Valencia, 46100 Burjassot (Valencia), Spain, and Fachbereich Chemie der Universität Marburg, Hans-Meerwein-Strasse, D-3550 Marburg, West Germany

$Cu(terpy)X_2$ ($X = Br^-, NCS^-$): Complexes with an Unusual Five-Coordination. Structural and Spectroscopic Investigation

M. I. Arriortua,[†] J. L. Mesa,[†] T. Rojo,*[,†] T. Debaerdemaeker,[‡] D. Beltrán-Porter,[§] H. Stratemeier,[∥] and D. Reinen*[,∥]

Received May 19, 1987

The structures of the five-coordinate complexes $Cu(terpy)X_2$ [X = NCS^- (I), Br^- (II)] were determined (monoclinic, space group $C2/c$, $Z = 4$). The unit cell dimensions are $a = 13.724$ (3) [16.818 (3)] Å, $b = 9.501$ (1) [9.280 (10)] Å, $c = 14.187$ (3) [11.396 (7)] Å, $\beta = 110.54$ (2)° [125.61 (4)°] for I [II], respectively. The unusual molecular geometry can be understood by following the pathway of the three ϵ' normal modes in D_{3h} symmetry. While usually the pathway leads from the compressed trigonal bipyramid into the elongated square pyramid as the energetically slightly preferred coordination, in these cases a geometry is observed that results from ligand movements in the "reverse" direction. Single-crystal EPR measurements confirmed the structural results and excluded the possibility of a dynamically averaged geometry. In frozen solution a conformational change to a square pyramid occurs.

Introduction

It has been shown that d^9-configured cations in a chemical environment of five equal ligands tend to stabilize either a compressed trigonal bipyramid or an apically elongated square pyramid with obviously an energetic preference for the latter coordination.[1] Symmetry considerations, based on vibronic interactions between the A_1' ground state and the first excited E' state in D_{3h} via the three ϵ' modes (pseudo-Jahn–Teller effect),[2] stereochemical results, and angular-overlap energies derived from the electronic spectra were used for the calculation of the ground-state potential surface.[3] Three rather flat minima result, which correspond to the three square-pyramidal conformations depicted in Figure 1. The presence of different ligands, rigidity effects of polydentate ligands, or packing effects in the unit cell may modify the potential surface, induced by the pseudo-Jahn–Teller coupling, however, and generate energy minima for geometries different from those just mentioned. The terpyridine ligand in complexes $Cu(terpy)X_2 \cdot nH_2O$ is interesting in this respect, because it imposes considerable angular distortions and bond length strains on the system. While in $Cu(terpy)Cl_2 \cdot nH_2O$ ($n = 0$ and 1),[4,5] in $Cu(terpy)(NO_2)_2 \cdot H_2O$,[6] and in $Cu(terpy)(NO_2)(NO_3) \cdot 2H_2O$[7] Cu^{2+} is found in a distorted square pyramid, with the terpyridine ligand in the equatorial plane, the title compounds $Cu(terpy)(NCS)_2$ and $Cu(terpy)Br_2$ exhibit a quite unusual coordination geometry in the solid state. The crystal structures and spectroscopic properties are described in this work and will be discussed by utilizing the vibronic coupling with the trigonal-bipyramidal ϵ' normal vibrations.

Experimental Section

Preparation of the Compounds $[Cu(terpy)X_2]$ ($X = Br^-, NCS^-$). **$X = Br^-$.** This compound was synthesized by a method different from the one described in literature.[4] A solution of $CuBr_2$ in ethanol (0.86 mmol in 10 mL) was mixed with an ethanol solution containing a stoichiometric amt. of 2,2':6',2''-terpyridine (0.86 mmol in 15 mL). The microcrystalline green precipitate was washed with ether and recrystallized from a water/ethanol solution. Anal. Found (calcd) for $C_{15}H_{11}N_3Br_2Cu$: C, 39.3 (39.4); N, 9.3 (9.2); H, 2.2 (2.4); Cu, 13.8 (13.9).

$X = NCS^-$. Diluted solutions of $CuCl_2 \cdot 2H_2O$ in water and terpyridine in ethanol were mixed in a 1:1 molar ratio. The resulting solution was treated with a slight excess of KNCS to give a green precipitate. It was filtered, washed with water, and recrystallized from a water/ethanol solution. Anal. Found (calcd) for $C_{17}H_{11}N_5S_2Cu$: C, 49.5 (49.4); N, 17.2 (17.0); H, 2.6 (2.7); Cu, 15.4 (15.4).

Spectroscopic Measurements. The ligand field reflection spectra were recorded by a Zeiss PMQII spectrometer (Infrasil) with a low-temperature attachment. We used Sr_2ZnTeO_6 (4000–12000 cm^{-1}) and freshly sintered MgO (8000–30000 cm^{-1}) as standards. The EPR spectra were taken with a Varian E 15 spectrometer (35 and 9 GHz) at 298, 77, and 4.2 K. DPPH was used as internal standard ($g = 2.003_7$).

X-ray Structure Determination. Single crystals of the compounds $[Cu(terpy)Br_2]$ and $[Cu(terpy)(NCS)_2]$, with dimensions 0.5 × 0.04 × 0.02 and 0.35 × 0.14 × 0.11 mm, respectively, were used for crystal data and intensity data collection. Oscillation and Weissenberg photographs were applied to determine the crystal systems. Systematic absences hkl ($h + k = 2n$) and $h0l$ ($l = 2n$) indicated that the possible space groups are Cc or $C2/c$ for both complexes. Diffraction data were collected at room temperature on a Philips PW 1100 automated diffractometer, using graphite-monochromated Mo Kα radiation (λ = 0.7107 Å). Physical properties and parameters pertinent to data collection, structure solution, and refinements are reported in Table I.

$X = Br^-$. Lattice constants were obtained by a least-squares fit of 30 reflections in the range $4° < 2\theta < 50°$. Intensities of three standard reflections were measured every 90 min and did not exhibit any significant variations in their intensities during data collection. Correction for Lorentz and polarization effects were applied. Direct methods (MULTAN

[†] Universidad del Pais Vasco.
[‡] Universität Ulm.
[§] Universidad de Valencia.
[∥] Universität Marburg.

(1) Reinen, D.; Friebel, C. *Inorg. Chem.* **1984**, *23*, 791.
(2) Pearson, R. G. *Symmetry Rules for Chemical Reactions*; Wiley-Interscience: New York, 1976.
(3) Reinen, D.; Atanasov, M.; Stratemeier, H. to be submitted for publication.
(4) Henke, W.; Kremer, S.; Reinen, D. *Inorg. Chem.* **1983**, *22*, 2858.
(5) Rojo, T.; Vlasse, M.; Beltran-Porter, D. *Acta Crystallogr., Sect. C: Cryst. Struct. Commun.* **1983**, *C39*, 194.
(6) Allmann, R.; Kremer, S.; Kucharczyk, D. *Inorg. Chim. Acta* **1984**, *85*, L19.
(7) Savariault, J. M.; Rojo, T.; Arriortua, M. I.; Galy, J. *C. R. Seances Acad. Sci., Ser. 2* **1983**, *297*, 895.

0020-1669/88/1327-2976$01.50/0